Biosensors and Bioelectronics xxx (2010) xxx–xxx

Contents lists available at ScienceDirect

Biosensors and Bioelectronics

journal homepage: www.elsevier.com/locate/bios

Detection of effect of chemotherapeutic agents to cancer cells on gold nanoflower patterned substrate using surface-enhanced Raman scattering and cyclic voltammetry

Waleed Ahmed El-Said [a], Tae-Hyung Kim [b], Hyuncheol Kim [a,b], Jeong-Woo Choi [a,b,*]

[a] Interdisciplinary Program of Integrated Biotechnology, Sogang University, #1 Shinsu-Dong, Mapo-Gu, Seoul 121-742, Republic of Korea
[b] Department of Chemical & Biomolecular Engineering, Sogang University, #1 Shinsu-Dong, Mapo-Gu, Seoul 121-742, Republic of Korea

ARTICLE INFO

Article history:
Received 14 April 2010
Received in revised form 12 July 2010
Accepted 22 July 2010
Available online xxx

Keywords:
Raman spectroscopy
SERS
HepG2 cell
Gold nanoflower
Nanobiochip
Drug discovery

ABSTRACT

In vitro assays have generally been carried out for cytological diagnosis and for evaluation of the cytotoxic effect of chemotherapeutic agents as an alternative to animal experiments. In this study, a method for fabrication and application of a gold nanoflower array on an ITO substrate for evaluation of the effect of chemotherapeutic agents on cancer cell behavior by the surface-enhanced Raman scattering (SERS) analysis, as well as the electrochemical detection was described. Due to the increased sensitivity provided by gold nanoflower substrates, the effect of chemotherapeutic agents at low concentration level was successfully detected based on SERS technique. This substrate was found to give enhanced Raman spectra with high surface plasmon field in the near infrared (NIR) spectral range, which minimize fluorescence interference and photo-toxicity. Cyclic voltammetry (CV) was further performed for confirmation of results obtained by SERS assay and showed increased intensity of current peaks for various concentrations at low levels. The developed Au nanoflowers modified ITO substrates developed in this study could be used as a simultaneous SERS and CV substrate to determine the effects of chemotherapeutic agents on cancer cells.

1. Introduction

There has been considerable interest in development of highly sensitive and selective methods for monitoring of the effect of anticancer drugs with short detection time, leading to development of many cell-based assays for effective detection of cell viability (Choi et al., 2004). Optical and spectroscopic methods including counting assay, MTT (3-(4,5-dimethylthiazol-2-yl)-2,5-diphenyltetrazolium bromide) assay (Liu et al., 2009), apoptosis enzyme-linked immunosorbent (ELISA) assay (Frankfurt and Krishan, 2003), spectrophotometric methods (Sankar et al., 2003), fluorescent microscopy (Fohlerová et al., 2007) or confocal microscopy (Prasad and Quijano, 2006) have been widely used for clarification of the exact relationship between cells and drugs or toxins. Although these optical and spectroscopic methods have provided reliable and reproducible results for detection of cell viability, complicated sampling procedures are required due to the necessity for exogenous fluorophores that provide only limited cellular information. Non-optical methods based on electrochemical tools such as electrochemical impedence spectroscopy (EIS), amperometry, and cyclic voltammetry (CV) which can detect the cell viability without fluorescence dyes, have been developed (Arndt et al., 2004; Karasinski et al., 2005; Kaya et al., 2003; Thielecke et al., 2001). In our previous work, viability changes of HeLa and HepG2 cancer cells exposed to anticancer drugs were successfully analyzed using cyclic voltammetric technique (El-Said et al., 2009a,b). However, because the current peak from cyclic voltammetry represents cell viability only via electron transfer between cell and electrode surface, different effects of various kinds of drugs on cancer cells cannot be monitored by electrochemical methods (Yea et al., 2007).

Raman spectroscopy is a powerful analytical technique that enables a rapid, reagent-free and non-destructive analysis of living cells (Thomas, 1999). The fundamental principle of this spectroscopic technique is based on the inelastic scattering of photons from molecules in the sample activated by the laser source. Hence, biochemical composition of cells can be thoroughly studied by analysis of each peak from Raman spectra, which is not available with other optical, biological or electrical methods (Smith and Dent, 2005). A number of studies have reported on Raman spectroscopy as a tool for cell analysis these include examination of cell populations in suspension (Short et al., 2005; Krishna et al., 2006), single fixed cells (Krafft et al., 2005), dried cells (Schuster et al., 2000), cytospun cells

* Corresponding author at: Department of Chemical and Biomolecular Engineering, Sogang University, #1 Shinsu-Dong, Mapo-Gu, Seoul 121-742, Republic of Korea. Tel.: +82 2 705 8480; fax: +82 2 3273 0331.
E-mail address: jwchoi@sogang.ac.kr (J.-W. Choi).

0956-5663/$ – see front matter © 2010 Elsevier B.V. All rights reserved.
doi:10.1016/j.bios.2010.07.089

(Crow et al., 2005), and living and dead cells (Notingher et al., 2002). Raman spectroscopy as a candidate for studying the effects of different anticancer drugs on cell viability has greeted very promise, due to the fact that different toxic agents or drugs will cause different effects on living cells and further induce changes in biochemical composition, which can readily be detected by Raman spectra without invasive procedures. However, application of Raman spectroscopy to cell-based analysis is very limited due to its weak and unstable signal.

Surface-enhanced Raman scattering (SERS) phenomenon offers an exciting opportunity to overcome the critical disadvantages of this normal Raman spectroscopy. Using the SERS technique, the Raman signal is enhanced by the structured metal surface and can be detected effectively by low laser power with short signal acquisition time available for biological applications (Volkan et al., 2000). Electromagnetic field enhancement "field enhancement" has been reported as one of the major SERS enhancement mechanisms. Field enhancement occurred at the surface of metallic nanoparticles (NPs) as a consequence of the interaction between laser radiation and electrons on the metal surface for activation of surface plasmons or collective oscillations of metal electrons. Aggregation of metallic NPs has been reported to generate very intense and enhanced Raman signals at the junction between two NPs, which are normally called 'hot spots' (Jiang et al., 2003).

For this reason, a great deal of attention has been focused on synthesis of shape-controlled SERS structures with different morphologies including spherical gold (Au) NPs, nanospheres, nanorods or nanostars for examination of their Raman enhancing capabilities, which are greatly influenced by their shape (Orendorff et al., 2006; Tiwari et al., 2007). However, fabrication of SERS-active substrates was found to have a number of problems, including poor signal enhancement, uniformity or reproducibility and further process for removal of the template and byproducts. Therefore, an advanced method for fabrication of the SERS-active surface is still required for more effective enhancement of Raman signals.

Here, we report on a simple, one step and template-free method for fabrication of a highly sensitive Au nanoflower modified ITO substrate and its applications for monitoring the effects of three different anticancer drugs on HepG2 cell. Au nanoflower array modified ITO substrate was developed based on electrochemical deposition of Au from Au^{3+} solution in presence of polyethylene glycol (PEG) as a surfactant on an ITO surface. This Au nanoflower deposited ITO substrate has shown a broad absorption band from the visible to the NIR region. Since the NIR laser is fluorescence free and can also penetrate much deeper into the sample, biochemical composition and/or its variance can be analyzed more effectively without cellular damages. Living HepG2 cells were immobilized on an Au nanoflower patterned ITO substrate for use as a cell-based chip for study of the various effects of anticancer drugs on cell viability depending on differing action mechanisms. Due to significant signal enhancement provided by the Au nanoflower deposited ITO substrate, the effects of anticancer drugs at low concentration level on target cells can be successfully detected using a SERS technique, which was validated using an electrochemical method.

2. Materials and methods

2.1. Materials

Hydrogen tetrachloroaurate (III) trihydrate ($HAuCl_4{\cdot}3H_2O$, 99.9+ %), 5-fluorouracil, 11-mercaptoundecanoic acid (MUA), and phosphate buffered saline (PBS) (pH 7.4, 10 mM) solution were purchased from Sigma–Aldrich (St. Louis, MO, USA). Hydroxyurea and cyclophosphamide monohydrate were purchased from Calbiochem (Germany). Polyethylene Glycol (PEG, MW = 200) was obtained from Yakuri Pure Chemicals Co. Ltd. (Osaka, Japan). All other chemicals used in this study were obtained commercially as reagent grade.

2.2. Cell culture

HepG2 cells collected from human liver were cultured in DMEM supplemented with 10% heat inactivated fetal bovine serum (FBS; Gibco, Carlsbad, CA, USA) and 1% antibiotics (Gibco). Cells were maintained under standard cell culture conditions at 37 °C in an atmosphere of 5% CO_2. The medium was changed every 2 days.

2.3. Electrochemical measurements

All electrochemical experiments were performed using a potentiostat (CHI-660, CH Instruments, USA) controlled by general-purpose electrochemical system software. A homemade three-electrode system consisted of an Au nanoflower coated ITO bottom as a working electrode, a platinum wire as the auxiliary electrode and Ag/AgCl as the reference electrode. Measurements were carried out to study the electrical properties of living cells and the effect of anticancer drugs on their behavior in normal laboratory conditions. PBS (10 mM, pH 7.4) was used as an electrolyte at a scan rate of 20 mV/s.

2.4. Fabrication of gold nanoflowers array modified ITO substrate

ITO-coated glass substrates were cleaned by sonication for 15 min using 1% Triton X-100 solution, deionized water (DIW) and ethanol sequentially, and then by basic piranha solution (1:1:5, H_2O_2:NH_3:H_2O) for 30 min at 80 °C. Finally, the substrates were cleaned by DIW and then dried under a N_2 stream to obtain a clean ITO surface. Au nanoflower arrays were electrochemically deposited on ITO substrates (20 mm × 10 mm) using a 0.5 mM $HAuCl_4$ aqueous solution containing PEG (20 μL/ml) as a surfactant. The potential was maintained at −1.3 V (vs. Ag/AgCl) and the deposition temperature was controlled for maintenance at 25 °C in an electric-heated thermostatic water bath. In order to remove any surfactant traces that may have been adsorbed on the Au nanoflower modified ITO surface, the substrates were rinsed in DIW and then boiled for 5 min with isopropyl alcohol. The active area for electrochemical deposition of Au nanoflowers was 10 mm × 10 mm, and their surface morphologies were analyzed by a scanning electron microscope (SEM) (ISI DS-130C, Akashi Co., Tokyo, Japan). A cell culture chamber unit with the dimensions of 1 cm × 1 cm × 1 cm (width × length × height) was attached to the Au nanoflower/ITO surface using polydimethylsiloxane (PDMS). Cells were transferred into the chip at a known cell density by infusion of new culture medium.

2.5. Raman spectroscopy

Biochemical composition of living HepG2 cells and the effect of chemotherapeutic agents on the cancer cells were investigated by Raman spectroscopy using Raman NTEGRA spectra (NT-MDT, Russia). The maximum scan-range, XYZ was 100 μm × 100 μm × 6 μm, and the resolution of the spectrometer in the XY plane was 200 nm and along the *Z* axis was 500 nm. Raman spectra were recorded using NIR laser emitting light at a 785 nm wavelength. Ten scans of 5 s from 600 cm^{-1} to 1700 cm^{-1} were recorded and the mean of these scans was used.

Please cite this article in press as: El-Said, W.A., et al., Biosens. Bioelectron. (2010), doi:10.1016/j.bios.2010.07.089

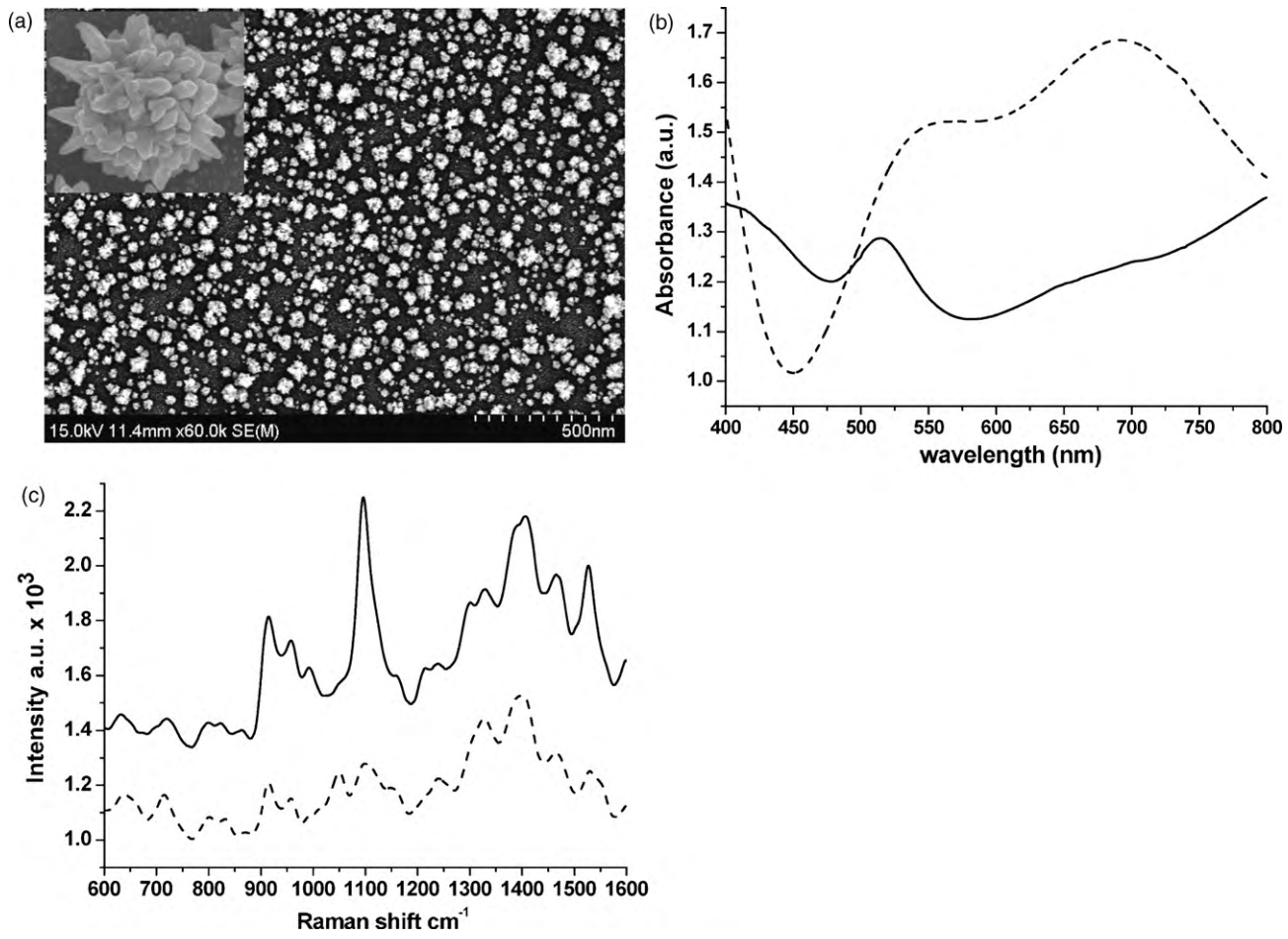

Fig. 1. (a) SEM topography of Au nanoflower array modified ITO substrate, inset SEM image of single Au nanoflower. (b) UV–vis spectra of (–) Au spherical nanoparticles/ITO and (– – –) Au nanoflower/ITO substrates. (c) SERS spectra of MUA immobilized on (–) Au nanoflowers/ITO and (– – –) Au nanoparticles/ITO substrates.

3. Results and discussion

3.1. Fabrication of gold nanoflower array modified ITO and its plasmon absorption

Au nanoflower arrays were fabricated by deposed of Au from Au^{3+} ions aqueous solution in the presence of PEG as a surfactant based on an electrochemical deposition method. Fig. 1a shows a topographic SEM image of the Au nanoflower array fabricated on the ITO surface representing a uniform distribution of nanoflowers with about diameter of 50–80 nm.

Recent studies have reported that surface plasmon absorption of the nanostructures change according to their size, shape, and composition (Link et al., 1999). Spherical Au NPs show an absorption band within the range from ac. 510 nm to 550 nm based on their size (Jain et al., 2006; Okamoto and Yamaguchi, 2003), while Au nanorods have two surface plasmon absorption bands in the visible and NIR regions at 515 nm and 680 nm, respectively (Link and El-Sayed, 2005; Muskens et al., 2008).

The absorption spectra of Au nanoparticles/ITO substrate demonstrated a weak surface plasmon absorption band within the visible region at 520 nm (Fig. 1b). However, Au nanoflowers/ITO substrate showed two surface plasmon absorption peaks; a strong broad peak in the NIR region (700 nm) due to longitudinal oscillation of the conduction band electrons, and a weak narrow wavelength band at around 540 nm contributed by transverse electronic oscillation. The longitudinal absorption band is more sensitivity to the local dielectric environment than the absorption band of spherical nanoparticles (Link and El-Sayed, 1999). Because the enhancement of surface electric field depends on the surface plasmon excitation, Au nanoflowers may strongly absorb the energy and scatter electromagnetic field. Moreover, the longitudinal absorption band of Au nanoflowers/ITO substrate (700 nm) overlapped with the excitation wavelength from a diode laser (785 nm), which may be another enhancement factor. Hence, we can expect that Au nanoflowers/ITO substrate may lead to a high enhancement of Raman signals compared to that of Au nanoparticles/ITO substrate.

In order to prove this, Raman signal of MUA layer self-assembled on both Au nanoflowers/ITO substrate and Au nanoparticles/ITO substrate were measured to compare the enhancement of Raman signal induced by the structural differences of Au deposited on ITO substrate (Fig. 1c). The result demonstrated that the MUA layer on Au nanoflowers/ITO substrate caused a significant increase of the intensity of the overall spectra (Fig. 1c). This result indicated that, the focus of the NIR laser on Au nanoflower arrays can induce strong surface plasmon effects and cause highly enhanced Raman scattering, which enables intensive SERS-based study of living cells without potential cell damage.

3.2. Raman spectra of living HepG2 cells

The SERS mechanisms were reported to involve two major enhancements (Campion and Kambhampati, 1998; Kneipp et al., 1999); an electromagnetic enhancement called as “electric effect” and the chemical enhancement called as “charge-transfer effect”. It

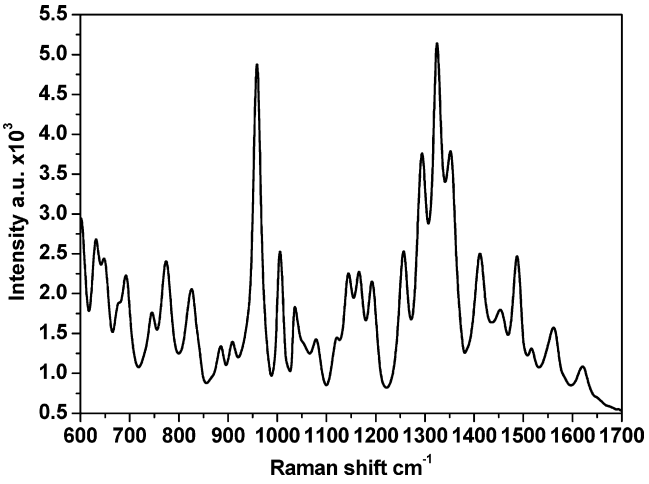

Fig. 2. SERS spectra of living HepG2 cells immobilized on an Au nanoflower array modified ITO.

was found that the electromagnetic enhancement plays as key role in the SERS effect (Otto et al., 1992).

The Au nanoflower structures with diameter of 50–80 nm are far more small compared to the wavelength of the excitation laser (785 nm), and hence allows the excitation of the Au nanoflower's surface plasmon which could be localized and increase the concentration of the electric field density. Due to the difference in dielectric constants between the Au nanoflowers surface and the surrounding media (Otto et al., 1992), the electromagnetic energy density on the Au nanoflowers could be a source for the electromagnetic enhancement that mainly contribute to SERS effect. Moreover, Au nanoflowers have high value of surface roughness due to its structural characteristics and finally induce the changes of electric field that can radiate both in a parallel and a perpendicular direction to the surface. So, if an incident photon falls on the roughened surface, the excitation of plasmon resonance of the metal may occur and will allow scattering.

Distribution of biopolymer in living HepG2 cells was studied using SERS spectra based on NIR laser (785 nm) within spectral range from 600 cm^{-1} to 1700 cm^{-1}. SERS spectra of living HepG2 cells consist of a series of bands corresponding to all biopolymers found in cells (Fig. 2). Nucleic acids can be identified by analysis of characteristic peaks corresponding to nucleotide and sugar-phosphate backbone vibrations. The main peaks are found at 1079 cm^{-1} (phosphodioxy group PO_2^-) and 824 cm^{-1} (–O–P–O– phosphodiester bonds in RNA). The spectra of proteins are dominated by peaks corresponding to Amide I (1620 cm^{-1}) and Amide III (1257 cm^{-1}) vibrations. Amino acids can be identified by peaks corresponding mainly to phenyl groups, such as phenylalanine (1006 cm^{-1}), tryptophan (772 cm^{-1}) and C–H vibrations (1452 cm^{-1}). Raman peaks of lipids are present at 1452 cm^{-1} and 1620 cm^{-1} (C=C stretching), and belong to vibrations of the hydrocarbon chains. Carbohydrates can also be detected by identification of Raman peaks of sugars, especially the C–O–C vibrations of the sugar rings (800–1450 cm^{-1}). The peak assignments of the spectra are presented in Table 1 (Xie et al., 2009).

Table 1
Peak assignments for living HepG2 cell SERS spectra.

Raman shift (cm^{-1})	Assignment
1620	Amide I, C=C Try, Trp
1560	Amide II, Trp
1485	G, A
1452	Deoxyribose: deformation (CH_2)
1413	Deoxyribose: stretching COO^-
1353	CH_3CH_2 twist
1323	G
1292	Lipid=CH bend, A, Pro.: CH def
1257	T, A, Pro.: Amide III β-sheet
1191	Nucleotides: base str. (CN)
1179	Pro.: Tyr, Phe
1152	Proteins: str. CN/CC
1120	Pro.: C–N str. deoxyribose: str. C–O
1079	Lipids, chain C–C str. deoxyribose: C–O, C–C str. Glycos. phosphate: str. PO_2^-
1033	Pro.: C–H in-plane Phe, deoxyribose: str. (CO)
1006	Pro.: sym. ring br Phe
960	Pro.: C–C str. α-helix
908	Pro.: ring str. (CC),
885	Deoxyribose: C–O–C ring
824	Phosphate: O–P–O str. RNA
772	U, C, T ring br.
748	T (ring breathing)
670	T, G
646	Tyr: CC twisting

3.3. Effect of different chemotherapeutic agents on Raman spectra of HepG2 cells

Different toxic chemotherapeutic agents have different effects on living cells and induce different biochemical changes in relation to cell death mechanisms. Detection of changes in biochemical composition of cancer cells based on Raman spectroscopy could overcome the limitations of the other biosensor techniques, which are limited with regard to detection and discrimination of a variety of toxic agents. Raman spectroscopy also has proven its ability for sensing molecular changes in cells exposed to anticancer drugs (Notingher et al., 2003; Verrier et al., 2004; Uzunbajakava et al., 2003).

Three different anticancer drugs (5-fluorouracil (5-FU), hydroxyurea (HU), and cyclophosphamide) were selected as representative anticancer drugs for the study of their different effects on HepG2 cancer cells based on SERS techniques using Au nanoflower modified ITO substrates as a SERS-active surface. 5-FU is a key inhibitor of the pathways involved in biosynthesis of pyrimidine and purine. Inhibition of these pathways leads to a decrease of building blocks for DNA, and finally effect DNA synthesis. So, the decrease in the relative intensity of Raman bands corresponding to DNA bases (Raman shifts at 646 cm^{-1}, 1323 cm^{-1} and 1485 cm^{-1}) can be expected due to the effects of 5-FU on cancer cells. HU is another effective inhibitor of DNA synthesis in HepG2 cells and leads to unbalanced growth and abnormal production of mRNAs and proteins (Hatse et al., 1999). So, the relative intensity values of the Raman peaks corresponding to RNAs and proteins as well as DNAs can be expected to decrease at the treatment of HU anticancer drug. Cyclophosphamide, a toxic nitrogen mustard derivative, is widely used in cancer chemotherapy, because its cross-links DNA double strands and leads to breakage of the DNA backbone, which result in severe mutations (Rua et al., 2000; Ren et al., 1999). Therefore, the treatment of cyclophosphamide may induce the decrease in the intensity of Raman peaks corresponding to DNAs as same as 5-FU does. In order to investigate the different responses from HepG2 cells after exposure to three kinds of drugs by the SERS technique, HepG2 cells were allowed to attach and grow for 24 h on Au nanoflower/ITO substrates, and fresh culture medium containing 1 mM of 5-FU, HU or cyclophosphamide was supplied; SERS signals were then measured after 24 h. The medium was removed and cells were washed three times with PBS, which will be used during SERS measuring for elimination of the effect of the medium on SERS signals. The measured Raman spectra represented that, many biochemical changes after treatment with anticancer drugs, and difference in biochemical composition was evident, particularly at Raman bands associated with DNA, RNA, proteins and

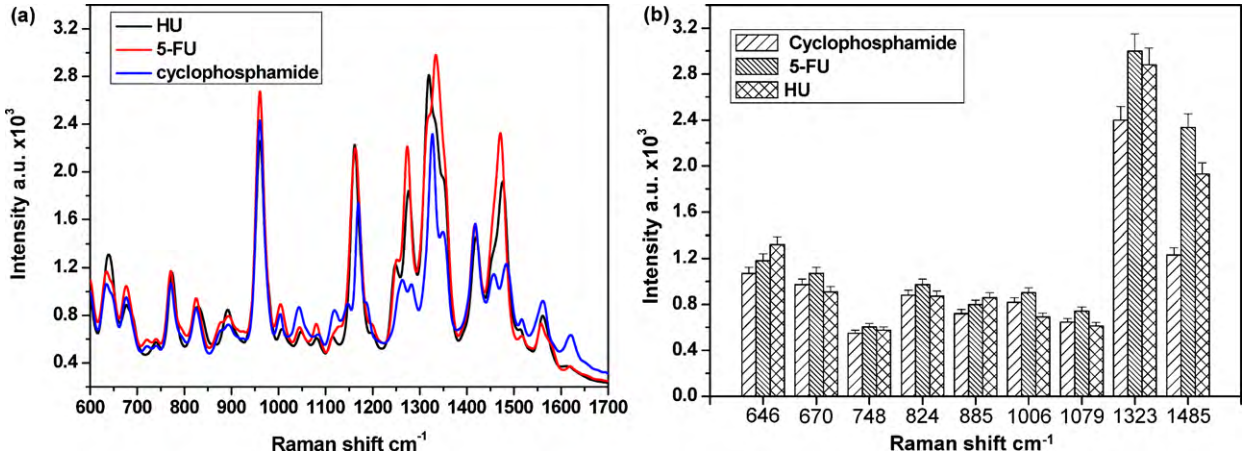

Fig. 3. (a) SERS spectra of living HepG2 cells exposed to 1 mM of hydroxyurea, 5-fluorouracil, and cyclophosphamide, cells were treated for 24 h. (b) Changes in biochemical contents of Raman peaks from HepG2 cells treated with 1 mM of cyclophosphamide, 5-fluorouracil, and hydroxyurea. Data represent the mean ± standard deviation of ten different experiments.

phospholipids. HU showed the highest effects due to its ability for inhibition of key steps in the pathways associated with pyrimidine biosynthesis that lead to inhibition of DNA synthesis. Fig. 3a shows that, the treatment of anticancer drugs results in the decrease in the relative intensities of Raman peaks at 670 cm^{-1}, 748 cm^{-1}, 1323 cm^{-1}, and 1485 cm^{-1}, corresponding to DNA bases as well as at 1079 cm^{-1} attributed to the O–P–O phosphodiester bonds. In addition, decreases in the relative intensities of Raman peaks, 1006 cm^{-1}, 1033 cm^{-1}, 1079 cm^{-1}, and 1292 cm^{-1}, corresponding to proteins were also observed. The decreased amount of proteins may be caused by the inhibition activity of anticancer drugs for DNA synthesis, because DNA is the original template for protein synthesis. These sequential inhibition activities of anticancer drugs finally lead to the cell death, which is detectable using Raman scattering due to the decrease of Raman active species. Raman spectra of HepG2 cell treated with cyclophosphamide showed a decrease of peak intensities assigned to phosphate and deoxyribose at 824 cm^{-1}, 885 cm^{-1}, 1079 cm^{-1}, 1452 cm^{-1} and 1485 cm^{-1}. The decrease of Raman peak was especially evident at spectral range from 1150 cm^{-1} to 1375 cm^{-1}, corresponding to proteins and lipids. Among the three different anticancer drugs tested here, 5-FU was found to give lowest effects on cancer cell viability refer to the Raman peaks at 646 cm^{-1}, 908 cm^{-1}, 1323 cm^{-1} and 1353 cm^{-1}, due to its specific inhibition mechanism which mainly block the DNA and RNA synthesis of cells in S-phase only. Because cell cycles cannot be synchronized without any additional treatment, cells in various phases will be less affected by 5-FU compared to the other drugs, and cause the least effects for decreasing the viability of cancer cells. Fig. 3b shows the intensities of Raman peaks corresponding to the changes of biochemical composition in HepG2 cells, which was treated with cyclophosphamide, 5-FU, and HU. These results completely match the previous studies focused on the mechanism of anticancer drugs (Scherf et al., 2000), hence proved the high sensitivity of Au nanoflower modified ITO substrate as a SERS-active surface which can be used as a effective tool for drug screening and drug discovery simply and sensitively.

3.4. Real time monitoring of the effects of anticancer drugs on HepG2 cells by Raman spectroscopy

Time-dependent effects of HU were monitored by analysis of biochemical changes in living HepG2 cells exposed to a 200 μM solution of HU for 24 h. Molecular mechanisms involved in cell death are represented by a decrease of Raman peaks associated with proteins and DNA (Fig. 4a). DNA disintegration of cells exposed to anticancer drug was detected by a decrease of peak intensity corresponding to phosphodiester bonds and by differences in backbone vibrations of DNA bases, such as the 772 cm^{-1} peak for –O–P–O– bond, as well as the DNA bases. Other spectral differences assigned to protein structures, such as phenylalanine at 1006 cm^{-1} and C–H deformation at 1323 cm^{-1} were also observed (Notingher et al., 2003; Verrier et al., 2004). These results demonstrated that our Au nanoflower array/ITO substrates could be used for development of cell-based biosensors for in situ monitoring of statistical effects of the drug exposure.

3.5. Cyclic voltammetry behavior of HepG2 cells

HepG2 cells at a density of 2.1×10^4 cell/ml, the same as for Raman detection, were seeded on the working electrodes (Au nanoflower/ITO and bare ITO electrode) for 2 days, and then exposed to the voltammetric assay for detection of redox properties of HepG2 cells, which may be related to redox enzymes in HepG2 cells, such as NADH dehydrogenase (ubiquinine) flavoprotein 2 and quinone oxidoreductase-like (QOH-1) (El-Said et al., 2009a,b). Fig. 5a and b shows cyclic voltammograms of HepG2 cells immobilized on bare ITO and Au nanoflower/ITO electrodes, respectively. HepG2 cells on the bare ITO electrode showed a weak cathodic peak at +0.04 V and an anodic peak at +0.15 V (Fig. 5a). On the other hand, HepG2 cells on the Au nanoflower/ITO electrode were found to give a very strong cathodic peak at +0.08 V and an anodic peak at +0.19 V (Fig. 5b). The Au nanoflower modified ITO electrode increased the active surface area for electron transfer, and hence increased sensitivity of CV compared to the bare ITO electrode. Increased sensitivity of the redox peak was approximately 194% higher than that of a bare ITO electrode.

3.6. Electrochemical detection of HepG2 cell proliferation and the effects of anticancer drugs

In order to study proliferation of HepG2 cells on the Au nanoflower/ITO surface using a CV assay, HepG2 cells were grown on Au nanoflower/ITO surfaces for 4 days. Proliferation rate was then determined based on CV measurement with respect to different incubation times. Fig. 5c shows the cyclic voltammograms of HepG2 cells after incubation for 2, 3 and 4 days, indicating that the current peak increased with respect to increase of incubation time related to cellular viability and proliferation.

After confirmation of the ability of CV assay for monitoring of cell viability, HepG2 cells treated with anticancer drugs to con-

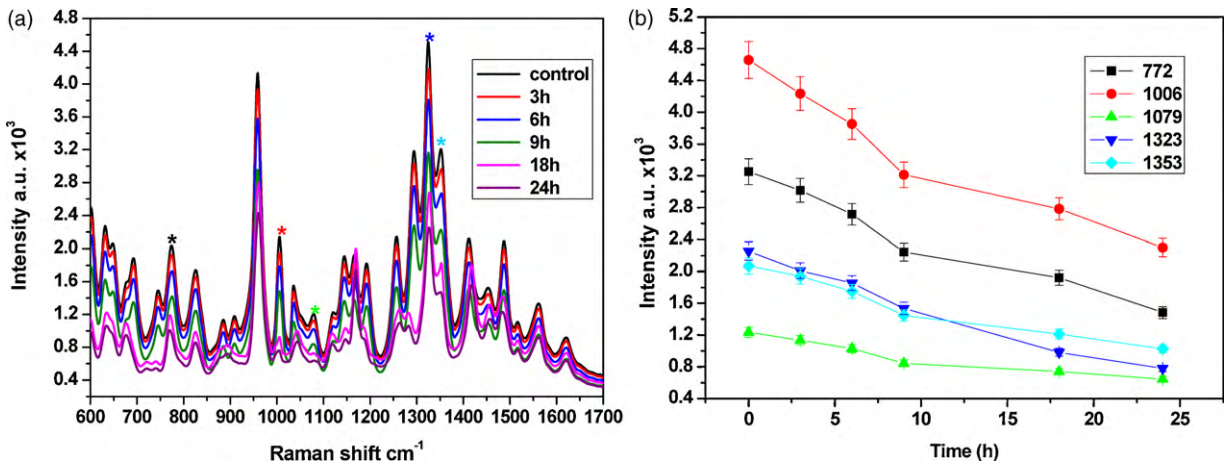

Fig. 4. (a) SERS spectra of HepG2 cells after treatment with 200 μM hydroxyurea for 3, 6, 9, 18 and 24 h. (b) Changes in DNA and protein contents of Raman peaks from HepG2 cells treated with 200 μM of hydroxyurea. Data represent the mean ± standard deviation of 10 different experiments.

firm the results of Raman spectroscopy, as well as its potential as a cell-based biosensor for screening the effect of drugs on cell viability. Living HepG2 cells were exposed to a low concentration of HU (200 μM), the same concentration, which used for Raman spectroscopy; CV was then measured with different treatment times. Fig. 5d showed voltammetric results from HepG2 cells before and after treated with 200 μM HU for 3, 6, 9, 18 and 24 h, representing the decreased current peak with increasing incubation time. The drop of current peak was evident corresponding to the increase of incubation time that represented the decrease of cell viability, however, not enough for explaining the chemotherapeutic action mechanism, which was available for Raman spectroscopy.

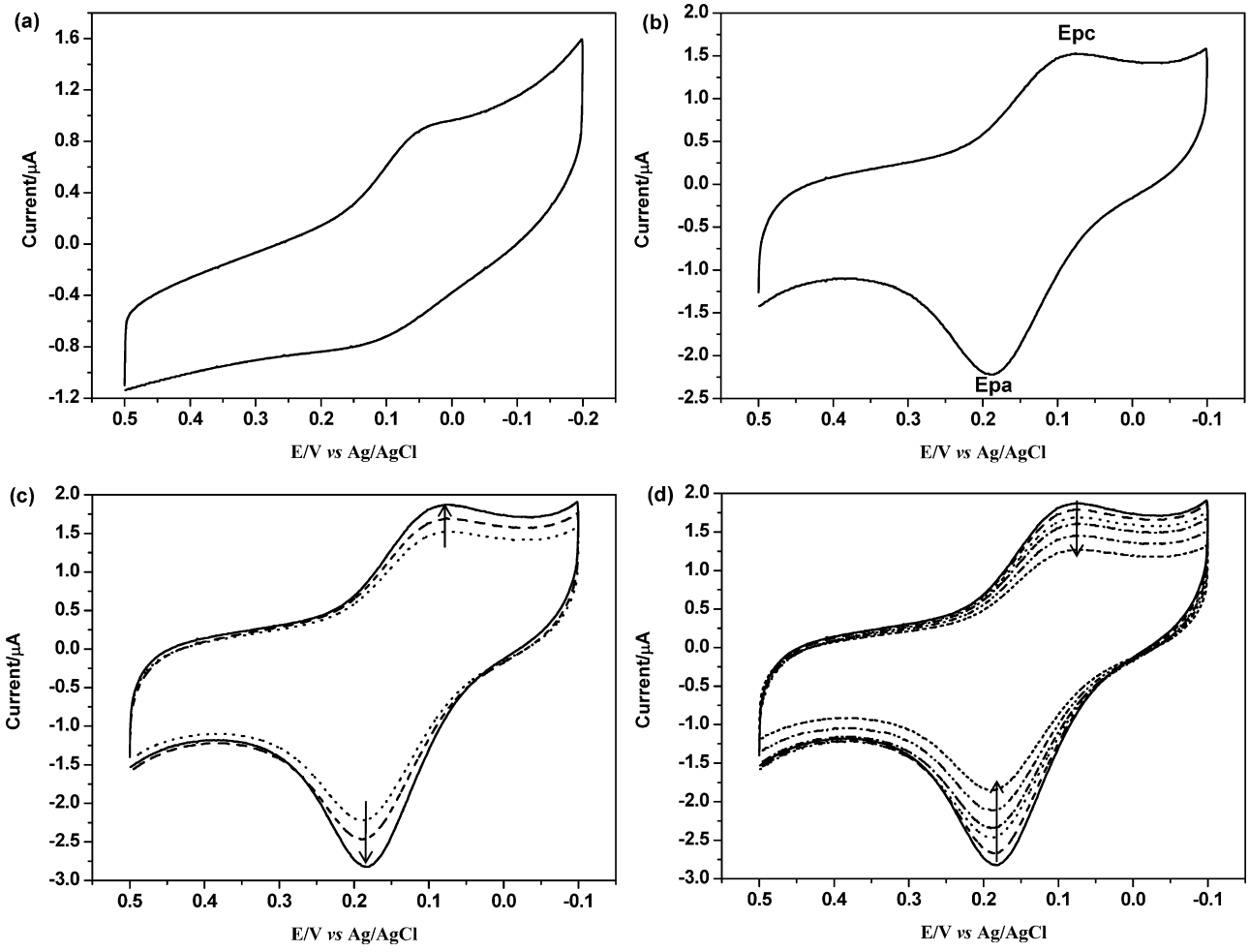

Fig. 5. Cyclic voltammograms of (a) Control HepG2 cells immobilized on a bare ITO electrode. (b) Control HepG2 cells immobilized on an Au nanoflower array modified ITO electrode. (c) HepG2 cells immobilized on an Au nanoflower array modified ITO electrode after incubating for 2 (. . .), 3 (– – –) and 4 days (–). (d) HepG2 cells immobilized on an Au nanoflower array modified ITO electrode, control HepG2 cells (–) and after treatment with 200 μM hydroxyurea for (– –) 3 h (– – –), 6 h (. . .), 9 h (– · – ·), 18 h (– · · –) and 24 h (– – –). The cell number was 2.1×10^4 cell/ml. Data represent the mean ± standard deviation of three different experiments.

Please cite this article in press as: El-Said, W.A., et al., Biosens. Bioelectron. (2010), doi:10.1016/j.bios.2010.07.089

4. Conclusions

In this study, we introduced a simple synthetic method for preparation of Au nanoflower modified ITO substrates by electrochemical deposition for enhancement of Raman signals from living cancer cells. The wavelength of the NIR laser was found to overlap with the wavelength for inducing the surface plasmon effects of the Au nanoflower array modified ITO surface, enabling sensitive detection of changes in biochemical composition in living cells without cellular damages in short detection time. Hence, the Au nanoflower modified ITO substrate was directly applied for detection of viability change in living HepG2 cells exposed to different kinds of anticancer drugs, and caused different effects for cells that were detectable using the SERS technique. Different effects of three kinds of anticancer drugs were successfully detected by analysis of each peak of the SERS signals; and anticancer drugs used in this study were found to have significant effects on the nucleus of HepG2 cells, especially for disintegration of DNA structure or prevention of its synthesis. These negative effects on cellular chromosomes led to decreased cell viability and/or proliferation, which were confirmed by cyclic voltammetry. Compared to bare ITO electrode, electrochemical signals from Au nanoflower modified ITO electrode also showed significantly increased signals, confirming its unlimited ability for enhancement of both optical and electrochemical signals from cells. Our study based on SERS and electrochemical techniques using Au nanoflower modified ITO substrate can be readily applied for sensitive in vitro drug screening with multiple detection and high sensitivity.

Acknowledgements

This work was supported by the National Research Foundation of Korea (NRF) grant funded by the Korean Government (MEST) (2010-0000845) and by the Nano/Bio science & Technology Program (M10536090001-05N3609-00110) of the Ministry of Education, Science and Technology (MEST) and by the Ministry of Environment of the Republic of Korea as "The Eco-technopia 21 project".

References

Arndt, S., Seebach, J., Psathaki, K., Galla, H.J., Wegener, J., 2004. Biosens. Bioelectron. 19, 583–594.
Campion, A., Kambhampati, P., 1998. Chem. Soc. Rev. 27, 241–250.
Choi, J.W., Nam, Y.S., Fujihira, M., 2004. Biotechnol. Bioprocess Eng. 9, 76–85.
Crow, P., Barrass, B., Kendall, C., Prieto, M.H., Wright, M., Persad, R., Stone, N., 2005. Br. J. Cancer 92, 2166–2170.
El-Said, W.A., Yea, C.-H., Kim, H., Oh, B.-K., Choi, J.W., 2009a. Biosens. Bioelectron. 24, 1259–1265.
El-Said, W.A., Yea, C.-H., Il-Keun, K., Choi, J.W., 2009b. Biochip J. 3, 105–112.
Fohlerová, Z., Skládal, P., Turánek, J., 2007. Biosens. Bioelectron. 22, 1896–1901.
Frankfurt, O.S., Krishan, A., 2003. Chem. -Biol. Interact. 145, 89–99.
Hatse, S., De Clercq, E., Balzarini, J., 1999. Biochem. Pharmacol. 58, 539–555.
Jain, P.K., Lee, K.S., El-Sayed, I.H., El-Sayed, M.A., 2006. J. Phys. Chem. B 110, 7238–7248.
Jiang, J., Bosnick, K., Maillard, M., Brus, L., 2003. J. Phys. Chem. B 107, 9964–9972.
Karasinski, J., Andreescu, S., Sadik, O.A., Lavine, B., Vora, M.N., 2005. Anal. Chem. 77, 7941–7949.
Kaya, T., Torisawa, Y., Oyamatsu, D., Nishizawa, M., Matsue, T., 2003. Biosens. Bioelectron. 18, 1379–1383.
Kneipp, K., Kneipp, H., Itzkan, I., Dasari, R.R., Feld, M.S., 1999. Chem. Rev. 99, 2957–2975.
Krafft, C., Knetschke, T., Funk, R.H.W., Salzer, R., 2005. Vib. Spectrosc. 38, 85–95.
Krishna, C.M., Kegelaer, G., ADT, I., Rubin, S., Kartha, V.B., Manfait, M., Sockalingum, G.D., 2006. Biopolymers 82, 462–470.
Link, S., El-Sayed, M.A., 1999. J. Phys. Chem. B 103, 8410–8426.
Link, S., El-Sayed, M.A., 2005. J. Phys. Chem. B 109, 10531–10532.
Link, S., Mohamed, M.B., El-Sayed, M.A., 1999. J. Phys. Chem. B 103, 3073–3077.
Liu, Q., Yu, J., Xiao, L., Tang, J.C.O., Zhang, Y., Wang, P., Yang, M., 2009. Biosens. Bioelectron. 24, 1305–1310.
Muskens, O.L., Bachelier, G., Del Fatti, N., Vallée, F., 2008. J. Phys. Chem. C 112, 8917–8921.
Notingher, I., Verrier, S., Haque, S., Polak, J.M., Hench, L.L., 2003. Biopolymers 72, 230–240.
Notingher, I., Verrier, S., Romanska, H., Bishop, A.E., Polak, J.M., Hench, L.L., 2002. Spectrosc. Int. J. 16, 43–51.
Okamoto, T., Yamaguchi, I., 2003. J. Phys. Chem. B 107, 10321–10324.
Orendorff, C.J., Gearheart, L., Jana, N.R., Murphy, C.J., 2006. Phys. Chem. Chem. Phys. 8, 165–170.
Otto, A., Mrozek, I., Grabhorn, H., Akermann, W., 1992. J Phys. Condens. Matter 4, 1143–1212.
Prasad, S., Quijano, J., 2006. Biosens. Bioelectron. 21, 1219–1229.
Ren, S., Kalhorn, T.F., Slattery, J.T., 1999. Drug Metab. Dispos. 27, 133–137.
Rua, Q.H., Luoa, G.A., Liaob, J.J., Liuc, Y., 2000. J. Chromatogr. A 894, 165–170.
Sankar, D.G., Kumar, J.M.R., Reddy, M.V.V.N., 2003. Asian J. Chem. 15, 1856–1858.
Scherf, U., Ross, D.T., Waltham, M., Smith, L.H., Lee, J.K., Tanabe, L., Kohn, K.W., Reinhold, W.C., Myers, T.G., Andrews, D.T., Scudiero, D.A., Eisen, M.B., Sausville, E.A., Pommier, Y., Botstein, D., Brown, P.O., Weinstein, J.N., 2000. Nat. Genet. 24, 236–244.
Schuster, K.C., Reese, I., Urlaub, E., Gapes, J.R., Lendl, B.B., 2000. Anal. Chem. 72, 5529–5534.
Short, K.W., Carpenter, S., Freyer, J.P., Mourant, J.R., 2005. Biophys. J. 88, 4274–4288.
Smith, W.E., Dent, G., 2005. Modern Raman Spectroscopy: A Practical Approach. John Wiley and Sons, Chichester.
Thielecke, H., Mack, A., Robitzki, A., 2001. Biosens. Bioelectron. 16, 261–269.
Thomas, G.J., 1999. Annu. Rev. Biomol. Struct. 28, 1–27.
Tiwari, V.S., Oleg, T., Darbha, G.K., Hardy, W., Singh, J.P., Ray, P.C., 2007. Chem. Phys. Lett. 446, 77–82.
Uzunbajakava, N., Lenferink, A., Kraan, Y., Willekens, B., Vrensen, G., Greve, J., Otto, C., 2003. Biopolymers 72, 1–9.
Verrier, S., Notingher, I., Polak, J.M., Hench, L.L., 2004. Biopolymers 74, 157–162.
Volkan, M., Stokes, D.L., Vo-Dinh, T., 2000. Appl. Spectrosc. 54, 1842–1848.
Xie, W., Wang, L., Zhang, Y., Su, L., Shen, A., Tan, J., Hu, J., 2009. Bioconjugate Chem. 20, 768–773.
Yea, C.-H., Min, J., Choi, J.-W., 2007. Biochip J. 1, 219–227.